In vitro immune responses of human PBMCs against Candida albicans reveals fungal and leucocyte phenotypes associated with fungal persistence

Nidia ALVAREZ RUEDA, Célia Rouges, Adel Touahri, Barbara Misme-Aucouturier, Marjorie Albassier, Patrice Le Pape

SCIENTIFIC REPORTS
nature research

OPEN

In vitro immune responses of human PBMCs against *Candida albicans* reveals fungal and leucocyte phenotypes associated with fungal persistence

Nidia Alvarez-Rueda*, Célia Rouges, Adel Touahri, Barbara Misme-Aucouturier, Marjorie Albassier & Patrice Le Pape*

Although there is a growing understanding of immunity against *Candida albicans*, efforts need to be pursued in order to decipher the cellular mechanisms leading to an uncontrolled immune response that eventually oppose disease eradication. We describe here significant intra- and inter-subject variations in immune response patterns of major human leucocyte subsets following an *in vitro* challenge with *C. albicans* clinical isolates. We also observed that there are *Candida* isolate-dependent changes in leucocyte phenotypes. Through a combination of multiple fungal growth and flow cytometric measurements, coupled to the tSNE algorithm, we showed that significant proliferation differences exist among *C. albicans* isolates, leading to the calculation of a strain specific persistent index. Despite substantial inter-subject differences in T cells and stability of myeloid cells at baseline, our experimental approach highlights substantial immune cell composition changes and cytokine secretion profiles after *C. albicans* challenge. The significant secretion of IL-17 by CD66+ cells, IFN-γ and IL-10 by CD4+ T cells 2 days after *C. albicans* challenge was associated with fungal control. Fungal persistence was associated with delayed secretion of IFN-γ, IL-17, IL-4, TNF-α and IL-10 by myeloid cells and IL-4 and TNF-α secretion by CD4+ and CD8+ T cells. Overall, this experimental and analytical approach is available for the monitoring of such fungal and human immune responses.

As a saprophytic organism, *Candida albicans* colonizes the human gastrointestinal, genitourinary and skin microbiota[1–3]. Healthy subjects conserve *C. albicans* in a commensal state through immune sensing, leading to the recognition of the fungus by specific receptors. The fungus co-exists with humans without causing damage, indicating the existence of evolutionary and adaptive fungal responses to immune mechanisms[3–6]. Despite human immune sensing, opportunistic invasive fungal infections (IFIs) due to *C. albicans* occur in patients with a diversity of immunological disorders and surrounded therapies[7–10]. These invasive infections represent an important public health challenge. Their incidence has been estimated to be between 1.5 to 8 per 100,000 global population, and their mortality rate remains very high (30–50%)[11–13].

A large amount of work has demonstrated that anti-fungal immunity requires the orchestration of innate immune responses followed by adaptive immune mechanisms[14–19]. Activation of innate monocytes and neutrophils depends on an adequate interaction with T lymphocytes[20]. *C. albicans* blastoconidia, hyphae and fungal antigens induce the recruitment of multiple immune cell populations around localized areas of infection. *Candida* infections could arise either from fungus-mediated damage or host-mediated immunity or both[21]. Hence, by initiating an inflammatory response, the delayed type of multicellular reaction during candidiasis could not only avoid fungal dissemination but also, in some cases, result in a deleterious hyperinflammatory response for the host. An excessive inflammatory reaction during candidiasis is primed by the secretion of a variety of inflammatory cytokines released through different kinetic patterns by specific tissue and blood cells. Like other infectious diseases, the multicellular inflammatory response can also be detrimental for humans and can contribute to

Nantes Université, CHU de Nantes, Cibles et médicaments des infections et du cancer, IICiMed, EA 1155, F-44000, Nantes, France. *email: nidia.alvarez-rueda@univ-nantes.fr; patrice.le-pape@univ-nantes.fr

fungal dissemination[22–25]. The most compelling evidence of a "dark side" of the immune reaction against *Candida* comes from clinical studies showing that a heightened inflammatory response induced by *C. albicans* occurs at the expense of host damage and pathogen eradication. Hence, the fungal pathogen induces a bidirectional influence between infection and immune-related pathology. For example, during chronic hepatosplenic disseminated candidiasis (CDC) and chronic mucocutaneous candidiasis diseases (CMCD), a local and systemic inflammatory reaction results in persistent infection[26–28]. The understanding of early immune events during systemic candidiasis has been considerably advanced by combining insights from different infection models. However, due to limited relevant experimental approaches for the study of immune responses under persistent conditions, relatively little is known about the kinetics of inflammatory events within the immune infiltrate microenvironment propitious to infection resolution or deleterious to the host. Efforts need to be pursued in order to decipher the cellular mechanisms leading to an uncontrolled immune response that eventually oppose disease eradication.

The capture of these dynamic and complex interactions strongly depends on the study design (cell line types, single vs. multicellular models, *Candida* species and time interaction). In our lab, we have developed an *in vitro* *Candida*-leucocyte co-culture model consisting of a delayed type of multicellular reaction after the challenge of human leucocytes by *Candida* species[29,30]. The analysis of the diversity of these immune responses is crucial to understand the pathophysiologic profiles implicated during fungal persistence. We conducted research about the dynamics of leucocyte populations in co-cultures associated with fungal elimination or persistence. We analysed leucocyte co-cultures to monitor the dynamics of immune and fungal cell interactions under persistent conditions. We have observed that *C. albicans* persists and proliferates into leucocyte cell co-cultures 6 days after challenge, despite the considerable candidacidal activity of human phagocytes during the first 2 days following infection. The analysis of immune responses highlighted that *Candida* persistence could result from an unbalanced production of pro-inflammatory cytokines, such as IL-6, IFN-γ and TNF-α, compared to anti-inflammatory IL-10 negative feedback, suggesting that, in some cases, the immune response is not effective against infection.

Recent results have been demonstrated the relevance of evaluating intra-*Candida* species variations and their influence during host-fungus interactions *in vivo*[31]. Furthermore, due to the natural individual variation of immune responses that could influence the fitness signatures in humans, we focused our analysis on a pilot prospective study including 16 healthy subjects to investigate the intra- and inter-variability of immune responses and fungal proliferation. For this purpose, immune responses from 16 healthy subjects were evaluated 2, 4, and 6 days after *in vitro* challenge by three different *C. albicans* clinical isolates to examine immune cell markers (CD3, CD4 and CD8 T lymphocytes and CD66 and CD14 myeloid cells) and cytokine secretion profiles (IFNγ, IL-17, IL-4, TNF-α and IL-10) by flow cytometry. Fungal burden was evaluated in parallel by retro-culture. The experimental design allowed the generation of multiplexed measurements consisting of flow cytometry and fungal growth data. We used the T-distributed Stochastic Neighbour Embedding (tSNE) algorithm to project and to analyse the structure of the neighbourhood and phenotype changes of the data. Previously, we reported the analytical approach of this model to characterize the responsiveness of a rare and poorly characterized immune population of double positive CD4+ CD8+ T cells against *C. albicans*[32]. In the present work, we provide raw components to infer *Candida* fitness in interactions with the major innate and adaptive human immune cells.

Results

Baseline variations of immune populations in healthy subjects before the challenge by *C. albicans*.

Peripheral leucocyte cells from 16 healthy volunteers were challenged by *C. albicans* after fresh leucocyte fraction separation by gradient centrifugation. The variation of immune phenotypes according to the intra- and inter-subject differences was followed by flow cytometry over a 3-month period. An independent blood sample was obtained monthly for each subject. We analysed the variation of immune parameters across subjects by combining the inter-subject baseline variability and temporal changes within subjects (intra-subject variability). After gating on total myeloid cells from region I, CD66+ cells (region II) and CD14+ (region III) cells were gated based on their expression markers. CD4+ and CD8+ T cells were analysed after gating on CD3+ T cell region IV (Fig. 1A).

We aimed to explore the performance of the tSNE algorithm for allowing the dimensional reduction and clustering of immune cell populations present in leucocytes from the same subject at three different time points. For that purpose, multiple baseline measurements were concatenated to generate a two-dimensional leucocyte differentiation map through a non-linear dimensional reduction tSNE analysis. Multiple flow cytometry measurements with a 5-color panel and viability dye from each subject over the 3-month period of sampling were used for clustering the following major immune cell subsets: CD14, CD66, CD3, CD4 and CD8. The outputs in Fig. 1B represent living PBMCs of 16 subjects at three different harvesting times before challenge by *C. albicans*. According to the expression marker, cells that are comparable were clustered together in space. This approach showed that each subject conserved specific cell composition signatures over time, which were highly variable between individuals. Figure 1C depicts the tSNE output of live leucocytes in a two-dimensional plot from 16 subjects on day 0. Despite the variability of cell phenotypes between subjects, this approach allowed the clustering of different immune populations according to the similarity of marker expression.

The examination of the major innate and adaptive PBMC frequency variations revealed a wide range of variance of CD4+ and CD8+ T lymphocytes on day 0 (Fig. 1D). While these T cells exhibited the highest variability among subjects (Fig. 1D, white boxes), they showed high within-subject stability (Fig. 1D, grey boxes). Interestingly, the total CD66+ neutrophil and CD14+ monocyte populations had minor temporal variations within subjects and were highly stable between subjects. Altogether, these data showed that a natural variation was present in the major immune cell populations in the group of 16 subjects.

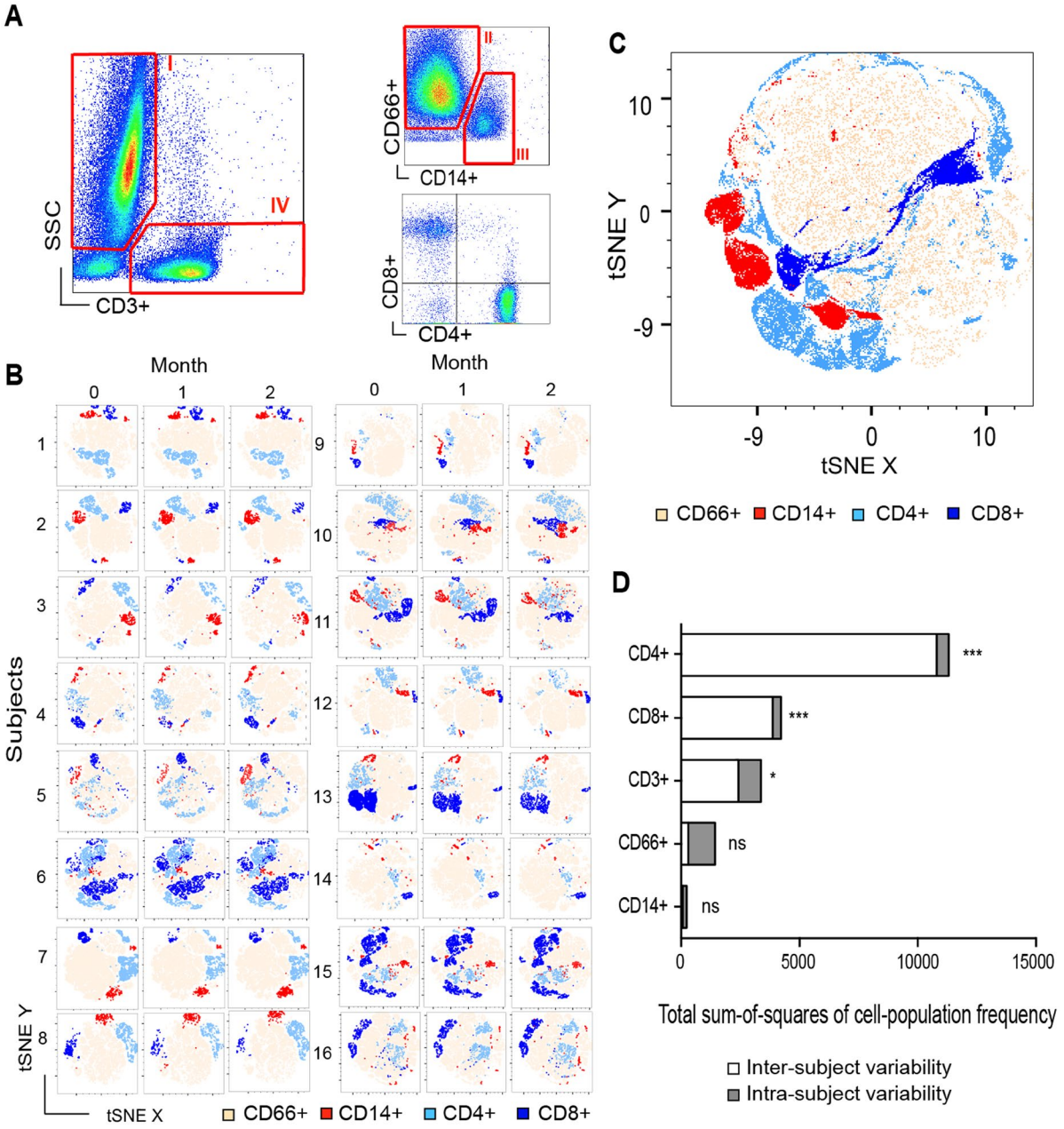

Figure 1. Intra- and inter-subject variation of immune cells at baseline. (**A**) Representative flow cytometry plots of the gating procedure for immune cells population characteristics. Fresh unstimulated leucocytes from each of the sixteen subjects were stained with specific antibodies. Plots show a side-scatter (SSC) versus CD3+ marker to gate human myeloid (I) and T lymphocytes (IV). Human CD66+ granulocytes and CD14+ cells were gated in the myeloid gate II and III, respectively. After gating on CD3+ T lymphocytes in gate IV, CD4+ and CD8+ T cells were separated based on the expression of single membrane markers. (**B**) Unsupervised clustering (tSNE) visualization of temporal immune cells phenotypic signatures among subjects. Two-dimensional tSNE (x, y) plots based on immune cells flow cytometry markers at baseline of 16 subjects and reconstitution of cell frequency and phenotypic similarity for CD66+ (beige), CD14+ (red), CD4+ (light blue), CD8+ (dark blue). Data are representative of three independent experiments for each subject, each in duplicate. (**C**) Global tSNE visualization of immune cells phenotypes at baseline. Downsampling function of multiple inter-subject measurements was applied before data concatenation. The resulting FCS file was analyzed on FlowJo tSNE module to reconstitute a single two-dimensional plot gathering the phenotypic similitudes of immune cells from among subjects ($n = 16$). (**D**) Variation in CD4+, CD8+, CD3+, CD66+ and CD14+ cell subpopulation frequencies at baseline. The relative contribution of inter- versus intra-subject variability to the total observed variation in the immune parameters was measured by calculating the range of subject-to-subject differences. An Analysis of Variance Model (ANOVA) was fitted to assess what fraction of the observed frequency variance (expressed as sum-of-squares) is due to differences among subjects (inter-subject variability, white boxes) or temporal changes around the baseline within subjects (intra-subject variability, gray boxes). $p \leq 0.05$. $^{*}P < 0.05$; $^{**}P < 0.001$; $^{**}P < 0.0001$ by one-way ANOVA with Tukey's multiple-comparison test ($n = 16$). ns, not significant.

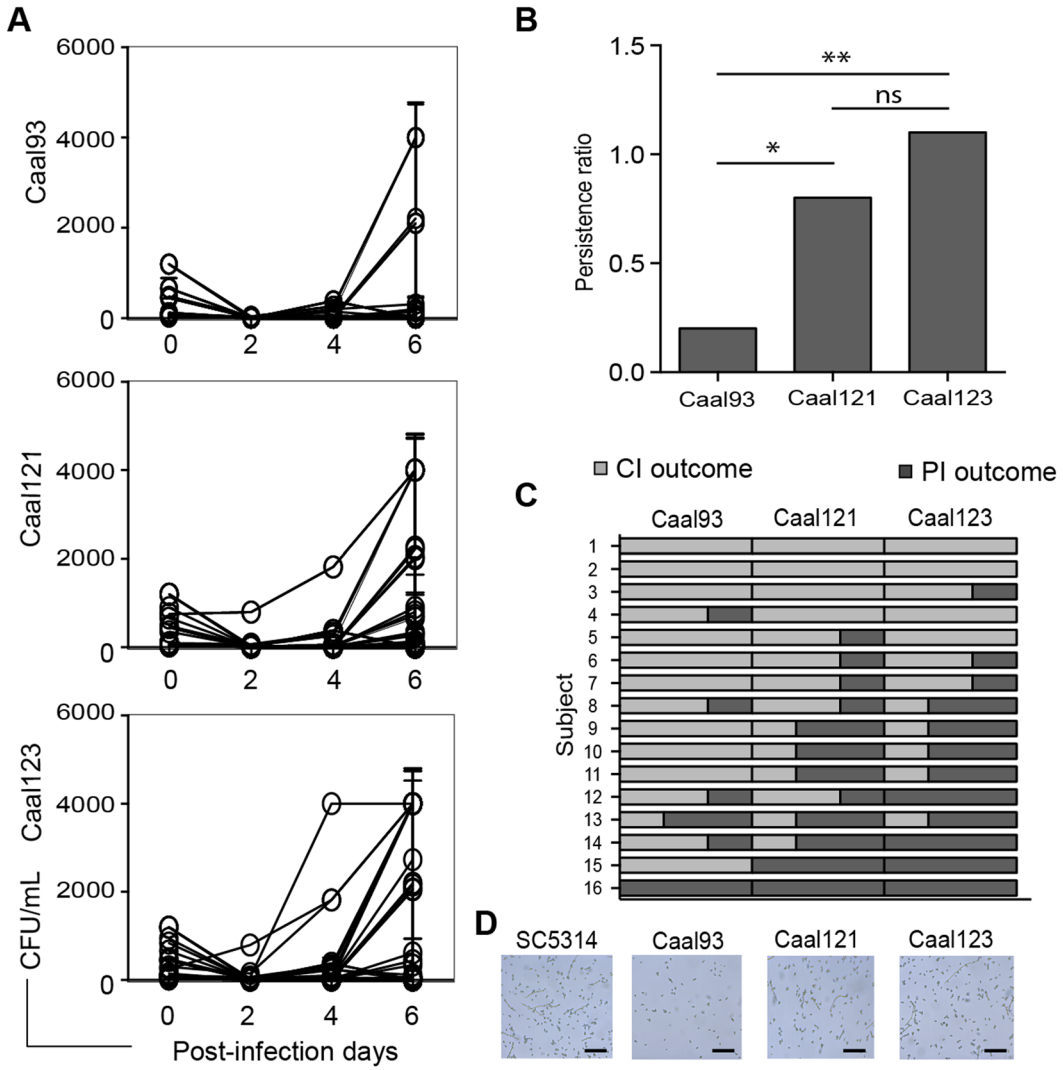

Figure 2. Proliferation of *C. albicans* into human leucocyte co-cultures. (**A**) Fresh human leucocytes were challenged by *C. albicans* clinical isolates (Caal93, Caal121 and Caal123). The candidacidal activity of leucocytes was measured on days 0, 2, 4, and 6 after challenge by retro-culture. Living cells were counted and fungal burden variation was expressed as the mean of colony-forming units (CFU/ml). Each curve depicts the mean ± SD of the growth evolution of each *C. albicans* clinical isolates of three separate experiments, each fungal load in duplicate ($n = 16$). (**B**) A fungal burden cutoff of 100 CFU/ml was applied on day 6 to summarize the resulting ability of each *C. albicans* isolate to proliferate into leucocyte cocultures from each subject. A controlled infection outcome (CI) corresponded to fungal burdens lower than this cutoff and persistent infection outcome (PI) were defined as higher than 100 CFU/ ml cutoff. The ratio of PI/CI for each clinical isolate was calculated by tacking the number of PI versus CI events for Caal93, Caal121 and Caal123 for all of subjects over the three months period. (**C**) Intra- and inter-subject variability of the response against *C. albicans* challenge. The arbitrary 100 CFU/ ml cutoff was applied to fungal burdens on day 6 post-challenge and the number of PI (dark gray) and CI (light gray) events for each subject over the three months period of sampling was expressed among Caal93, Caal121 and Caal123 ($n = 16$). (**D**) Light microscopic observation of morphologic characteristics of Caal93, Caal121, Caal123 and SC5314 control strain into axenic cultures of RPMI 1640 medium supplemented with 8% human serum (bars = 50 μm).

The proliferation of *C. albicans* clinical isolates into leucocyte co-cultures is characterized by specific persistence indexes. Leucocyte cells were challenged by three *C. albicans* strains. For each clinical isolate, the fungal growth was followed at different time points. The killing activity of human immune cells was measured by culturing living yeasts from co-cultures through a colony-counting technique. Results were expressed as the means of colony-forming unit (CFU/ml). Figure 2A depicts the CFU/ml means over the 6 days post-infection of PBMCs for each subject over the 3 months of sampling and each clinical isolate. The results showed a fungal burden reduction of the three *C. albicans* clinical isolates, Caal93, Caal121 and Caal123 2 days after challenge, reflecting the high candidacidal activity of phagocytes from all subjects. However, surviving yeasts were able to proliferate into leucocyte co-cultures, leading to a significant increase of the fungal burden

from the fourth to the sixth day after challenge. The resulting CFU/ml means 6 days after challenge were significantly different between the *C. albicans* isolates and were 492 ± 1188 (Caal93), 760 ± 1357 (Caal121) and 1490 ± 1811 (Caal123) CFU/ml ($p = 0.001$). Assessment of intra- and inter-subject comparisons demonstrated that subject-to-subject variability on day 6 contributed to the fungal load variation.

To further quantify these variations, we used a 100 CFU/ml cut-off to compare the proliferative ability of each *C. albicans* isolate into co-cultures 6 days after challenge. This cut-off is consistent with the CFU/ml mean used for leucocyte stimulation on day 0 (Fig. 2B). Fungal burdens lower than this cut-off were defined as controlled infection (CI, light grey), whereas fungal burdens higher than this cut-off were classified as persistent infection (PI, dark grey). Based on these criteria, we calculated a "persistence index", corresponding to the ratio of PI/CI for each clinical isolate (Fig. 2B). Interestingly, Caal121 and Caal123 showed a significantly higher persistence index compared to Caal93 ($p = 0.01$ and $p = 0.002$, respectively). Figure 2C shows a persistence map for each clinical isolate and subjects over the 3-month period of sampling. In addition to characteristics inherent to clinical isolates, we found that the ability of human leucocytes to control *C. albicans* infection was different between subjects. Among the 16 subjects, only 12.5% were able to clear the three clinical isolates over the 3-month period.

We next compared the axenic growth rates of isolates in order to explore the proliferation differences into leucocyte co-cultures. Under the same culture conditions, the generation times of the Caal93, Caal121 and Caal123 isolates were 8.2 ± 0.3 h, 7.1 ± 0.2 h and 6.4 ± 0.4 h, respectively, and were not significantly different from that of the SC5314 control strain (6.1 ± 0.2 h). Despite the absence of biofilm formation in RPMI 1640 medium supplemented with 8% human serum, microscopic observation of cultures revealed that the Caal121 and Caal123 isolates exhibited morphological differences, such as germ tubes and pseudohyphae formation after 4 h of culture at 37 °C and 5% CO2, which was similar to the SC5314 control strain (Fig. 2D).

tSNE analysis reveals *C. albicans*-induced changes in immune cell composition. *C. albicans*-leucocyte co-cultures induced immune aggregate reactions that were visible under light microscopy between days 4 and 6 after challenge (Fig. 3A). We focused the tSNE analysis on how *C. albicans* challenge could induce composition changes of immune cells. Figure 3B depicts two tSNE plots from one representative subject before and after challenge by the three clinical isolates. Compared to the baseline immune cell signature, challenge by every *C. albicans* isolate induced strong composition changes in immune cells on day 6 post-infection, which is illustrated by differences in clustering. Despite substantial baseline differences among subjects, *C. albicans* challenge induced clear coherent changes in CD14+, CD66+, CD4+ and CD8+ clustering. We also evaluated whether composition changes were specific for each clinical isolate or correlated with infection outcome. Hence, we fitted a tSNE analysis according to PI and CI outcomes and clinical isolates (Fig. 3C). By day 6, tSNE analysis showed that global profiles were similar among subjects and clinical isolates, but they were different regarding the infection outcomes (PI vs. CI). CD14+ expressing cells were highly clustered by tSNE under CI 6 days after challenge, while during PI, this cell subset could not be detected. tSNE also highlighted a coherent two-dimensional clustering of adaptive immune subsets (CD4+ and CD8+ cells) among *C. albicans* isolates and infection outcomes.

Leucocyte co-culture composition changes induced by *C. albicans* are consistent among subjects. We next evaluated whether immune variations could be due to the *C. albicans* strain used for the challenge or to inter-subject variability. To address this question, we fitted an ANOVA model to detect post-challenge changes in cell population frequencies compared to the pre-existing immune status on day 0. Figure 4A depicts the total sum-of-squares of immune population frequencies among *C. albicans* isolates and infection outcomes. Uninfected cells were used as controls. The global variance was composed by a first fraction corresponding to subject-to-subject variability (white boxes) and a second fraction explained by the *C. albicans* challenge variability (days 2, 4 and 6 after challenge, black boxes). Overall, *C. albicans* isolates did not induce significant changes in adaptive CD4+ and CD8+ T cell frequencies. This response was attributed to high stability of cell frequencies over the progression of post-challenge time and less subject-to-subject variability. However, when infection was controlled, the Caal93 and Caal121 isolates induced a significant variation in CD8+ T cells (Fig. 4A, CI). The innate CD66+ and CD14+ showed globally significant variations over the post-challenge time in all *Candida* isolates and for both CI and PI outcomes. Interestingly, these variations were consistent between the subjects.

Multiple flow cytometric measurements from all fungal isolates and subjects were concatenated in order to test the ability of tSNE to map composition changes induced after *C. albicans* challenge. Figure 4B shows dimensionality reduced data according to the infection status and the post-challenge time. The cellular occupancy of the resulting plots allows for coherent clustering of CD66+ and CD14+ cells, reflecting significant frequency diminutions. For adaptive CD4+ and CD8+ T cells, the tSNE plots were consistent with less significant frequency variations. We observed a slight separation of both CD4+ and CD8+ clusters, suggesting the presence of different T cell subsets over the time and according to the infection outcomes.

We next evaluated the origin of frequency variations over the post-challenge time (Fig. 4C). The PI and CI outcomes were compared to uninfected cell controls. Overall, day 2 responses included a significant reduction of CD66+ and CD14+ cells in both PI and CI groups compared to day 0. However, the percentage of CD66+ cells was significantly more reduced (31%) under PI compared to CI conditions and controls (23% and 19%, respectively; $p = 0.005$). The CD14+ cell frequencies were similar between the PI and CI conditions. Among CD3+ cells, CD4+ T lymphocytes were more abundant than CD8+ cells and had similar CD4+/CD8+ ratios between the CI and PI conditions (CI ratio of 3.5 and PI ratio of 3). By day 4, the diminution in the percentage of CD66+ cells continued in both groups but was significantly greater in the PI (56% by day 2 vs. 42% by day 4) compared to CI (63% by day 2 vs. 59% by day 4) and uninfected cells (64% on day 2 vs. 59% on day 4). Interestingly, CD14+ cell frequencies remained stable in CI outcomes compared to day 2. The CD4+/CD8+ increased in CI conditions

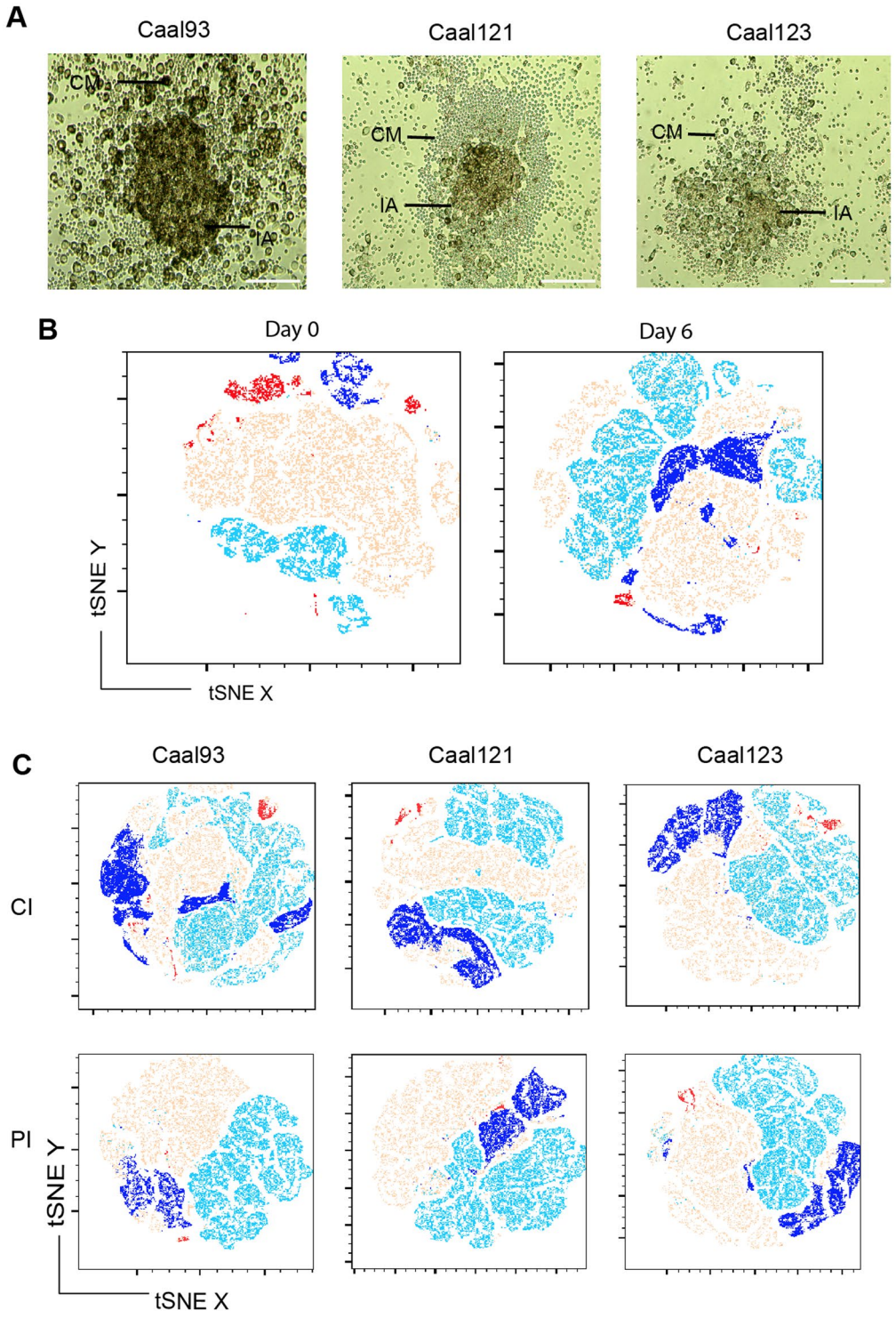

Figure 3. Phenotypic variations of human immune cells after *C. albicans* challenge. (**A**) Representative *C. albicans* immune-aggregates by light microscopy observation showing cell migration gradients (CM) and compact inflammatory aggregates (IA) 6 days after challenge with Caal93, Caal121 and Caal123 clinical isolates. Bars represent 50 μm. (**B**) Phenotypic modification of immune cells induced by *C. albicans*. Flow cytometry data from each subject over the three months period was concatenated and analyzed on tSNE FlowJo module. Representative unsupervised tSNE clustering of immune cells for one subject before (day 0) and after *C. albicans* challenge (day 6) showing phenotypic clustering of CD66+ (beige), CD14+ (red), CD4+ (light blue), CD8+ (dark blue) immune cells ($n = 16$). (**C**) tSNE phenotypic signatures induced in immune cells after challenge by Caal93, Caal121 and Caal123 clinical isolates according to CI outcome (fungal burdens lower than 100 CFU/ ml by day 6) and PI outcome (fungal burdens higher than 100 CFU/ ml by day 6). CD66+ (beige), CD14+ (red), CD4+ (light blue), CD8+ (dark blue) immune cells ($n = 16$).

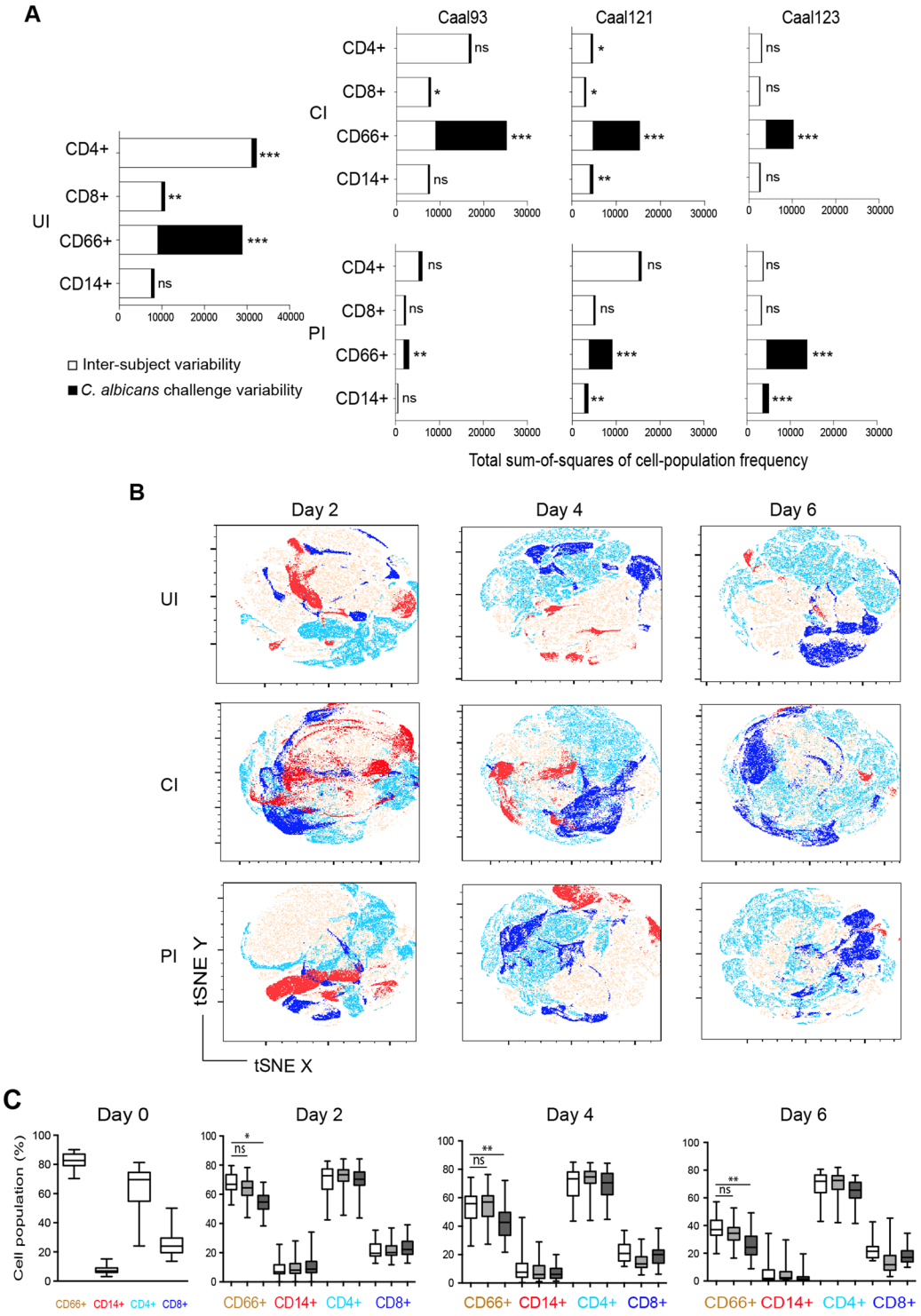

Figure 4. *C. albicans* post-challenge changes in the immune cell composition. (**A**) Variation in CD4+, CD8+, CD3+, CD66+ and CD14+ cell subpopulation frequencies after *C. albicans* challenge. An ANOVA model was fitted to assess what fraction of the observed variance of immune cell frequency is due to differences among subjects (inter-subject variability, white boxes) or to *C. albicans* challenge variability (black boxes) in comparison to unstimulated cells on day 0. The inter-subject variability was quantified within the columns as the sum of squares of differences between each subject and the sixteen subjects mean. The post-challenge variability was quantified as the sum of squares of the differences between the column means and the grand mean. The F ratio was the ratio of two sum of square values. Large F ratio signified higher post-challenge variability than inter-subject variability. The *P* value was determined from the F ratio and the two values of degrees of freedom. The relative contributions of inter-subject variability and *C. albicans* challenge to the total observed variation in the immune parameters was measured on Prism 6.0a by calculating the range of subject-to-subject differences (total sum-of-squares), $n = 16$, $p \leq 0.05$. Immune cells frequencies data were

analyzed according to UI controls, CI and PI outcomes for Caal93, Caal121 and Caal123 clinical isolates. (**B**) Global phenotypic modifications of immune cells induced by *C. albicans* over the post-challenge time. Data from all of subjects and clinical isolates were concatenated and analyzed on tSNE FlowJo module according to PI and CI outcomes and UI controls. Phenotype clustering shows CD66+ (beige), CD14+ (red), CD4+ (light blue), CD8+ (dark blue) immune cells expression. (**C**) Composition of *C. albicans* – leucocyte cocultures. The proportions of CD66+, CD14+, CD4+ and CD8+ cells were expressed as a percentage of the total living cell compartment. Box plots depict median, minimum, and maximum percentages of immune cells according to UI (white boxes) uninfected control, CI (light gray) and PI (dark gray) outcomes and on days 0, 2, 4 and 6 after challenge with *C. albicans*. $*P < 0.05$; $**P < 0.001$; $***P < 0.0001$ by one-way ANOVA with Tukey's multiple-comparison test ($n = 16$). ns, not significant.

at this time point. Day 6 responses primarily reflected changes in adaptive T cells, including an increase of the CD4+/CD8+ ratio in the CI outcome compared to the PI outcome (CI ratio of 4.7 and PI ratio of 3.4).

***C. albicans* induced functional post-challenge changes in immune cells.** Given previous results suggesting the presence of cell subsets, we next evaluated functional changes in immune cells consistent among subjects and associated with fungal persistence. We were particularly interested in evaluating the cytokine secretion profiles of specific innate and adaptive cells (myeloid cells and CD4+ and CD8+ T cells). Figure 5 shows the total sum-of-squares of cytokine secreting cell frequencies according to the cell population and to the infection outcome (PI and CI). Uninfected cells were used as controls (UI).

For uninfected cells, the total variance of all myeloid cell expressed cytokines was statistically significant. The inflammatory (IFN-γ, IL-17 and IL-4) and anti-inflammatory (IL-10) cytokines showed higher F ratios, suggesting significant *C. albicans* strain post-challenge variability (black boxes) over the inter-subject variability (Fig. 5, Table 1). Apart from IFN-γ and TNF-α, cytokine expression by CD4+ and CD8+ T cells did not significantly vary under uninfected conditions. Interestingly, the CI outcome was characterized by significant post-*C. albicans* challenge variability compared to uninfected cells, suggesting specific cytokine kinetics over the 6 days of incubation. The global variance of pro- and anti-inflammatory cytokines was significant and due to myeloid and CD4+ cytokine secretion. Myeloid cells showed high F ratios for TNF-α, IL-10 and IL-4, indicating that a major fraction of variation was due to *C. albicans* challenge variability. CD4+ T cells also showed high F ratios for TNF-α and IL-4. Under PI conditions, only myeloid cells induced significant variations in cytokine secretion (IFN-γ, TNFα and IL-10). As for CI conditions, the variance in cytokine secretion for the PI outcome was significantly provided from *C. albicans* variability (black boxes).

***C. albicans* persistence is associated with differential and delayed cytokine secretion kinetics.** We then asked whether post-challenge changes could be originating from differential cytokine secretion kinetics compared to uninfected cells. Using tSNE, we analysed the representation of flow cytometry measurements in terms of the global secretion of pro-inflammatory (IFN-γ) vs. anti-inflammatory (IL-10) cytokines according to the infection outcomes and the post-challenge incubation time. Consequently, tSNE generated a bicolour map showing the cytokine secretion kinetics (Fig. 6A). From this analysis, a marked secretion of pro-inflammatory cytokines by day 2 during CI conditions could be observed compared to the PI and UI outcomes. The anti-inflammatory cytokine kinetics were coherent with an earlier retro-control under CI compared to PI conditions. Figure 6B depicts the cytokine secreting cell frequencies according to UI, CI and PI outcomes. When *C. albicans* infection was controlled, pro-inflammatory cytokines (IFN-γ, TNF-α and IL-17) were secreted 2 days post-infection by significantly higher proportions, as compared to uninfected conditions. IFN-γ was significantly secreted by T cells. The frequency of CD4+ T cells secreting IFN-γ and TNF-α was significantly higher than CD8+ T cells (Fig. 6B,C). Interestingly, by day 2 after challenge, the secretion of IL-17 was significantly derived from myeloid cells, whereas we did not detect significant secretion levels of IL-17 by T cells. Among these cells, IL-17 was expressed by CD66+ neutrophils, principally after the challenge with Caal93, which was the less persistent isolate (Fig. 6D). IL-17 secretion by human CD66+ cells was then verified in a control experiment with sorted neutrophils stimulated with clinical isolates. Figure 6E depicts flow cytometry analysis of isolated neutrophils two days after challenge by *C. albicans*. Human neutrophils secreted significant proportions of IL-17 after challenge by Caal93, Caal121 and Caal123 as reflected by the higher fluorescence intensity ratios compared to isotype controls (1.9, 1.5 and 1.5, respectively). Results confirmed that isolated human neutrophils secreted IL-17 after stimulation with the less persistent clinical isolate Caal93 compared to uninfected controls. Il-17 was also secreted by CD66+ cells after challenge by the reference SC5314 strain (RFI of 1.7). Significant IL-17 concentrations were also detected in the supernatant of Caal93 and SC5314 stimulated neutrophils compared to uninfected controls (26 ± 3.1 pg/ml, 9.5 ± 4.4 pg/ml and 1 ± 0.5 pg/ml, respectively). IL-10 was also significantly secreted by day 2, mainly by CD4+ T cells (Fig. 6B,C). The kinetics of IL-4 was not significantly different under CI compared to uninfected cells. *C. albicans* persistence was characterized by the secretion of IFN-γ, TNF-α, IL-17, IL-4 and IL-10 cytokines by days 4 and 6 after challenge. These cytokines were principally secreted by myeloid cells. TNF-α and IL-4 secreting T cells were only significantly detected by days 4 and 6 after challenge compared to uninfected cells.

Discussion

During the host-*C. albicans* interaction, several parameters predispose to fungal disease, in particular *C. albicans* pathogenicity and host risk factors, such as immunosuppression (co-infections, immunosuppressive treatments and medical interventions)[4,33–35]. However, these factors alone do not fully explain why, under comparable risk factor conditions, only some patients develop infections[7–9]. Considering that *Candida* infections can be raised not

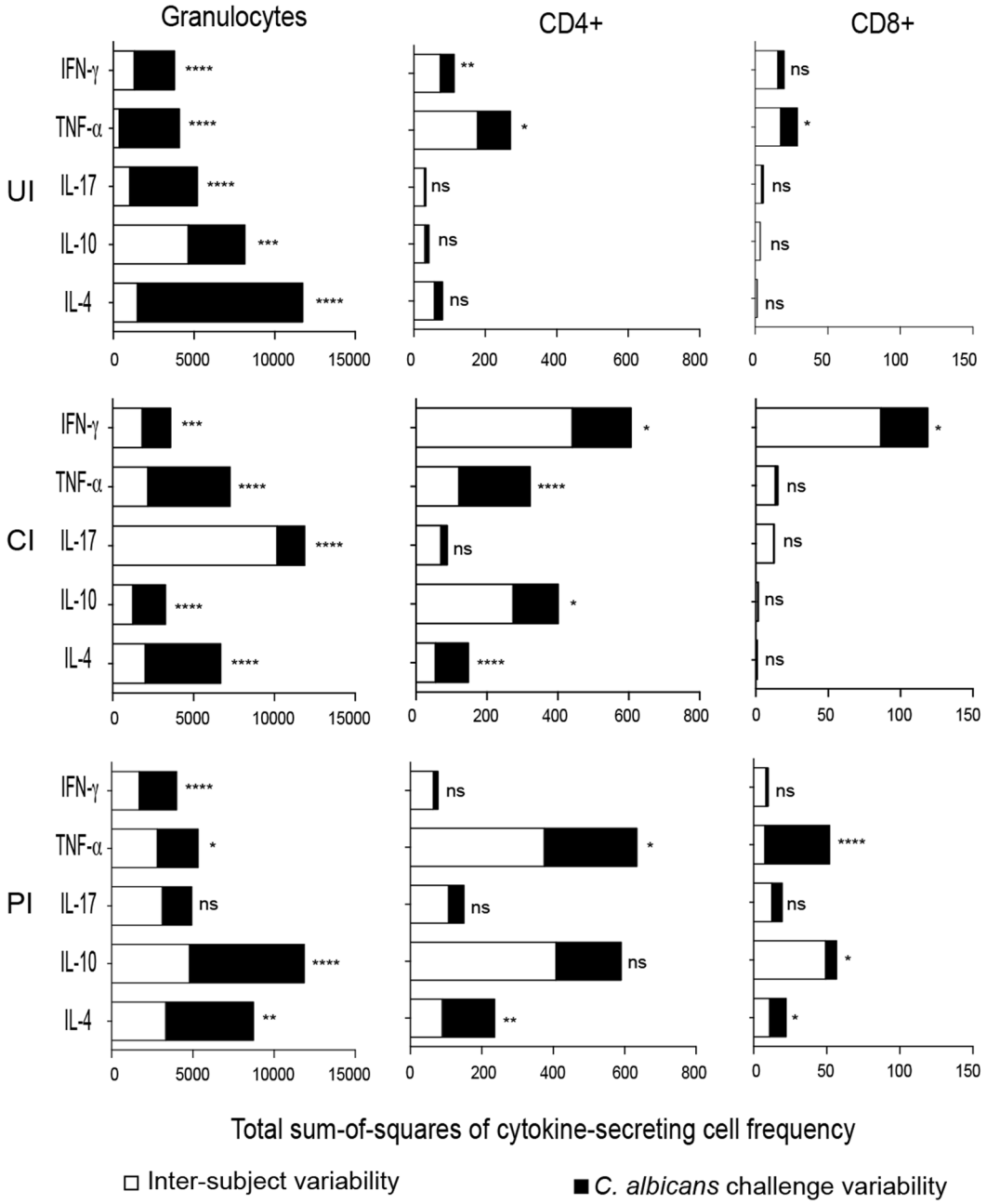

Figure 5. Variation of the cytokine secretion kinetics after *C. albicans* challenge. Unstimulated and *C. albicans*-stimulated leucocytes of sixteen subjects were stained for CD4+, CD8+ membrane-antibody markers and for IFN-γ, TNF-α, IL-17, IL-10 and IL-4 secreted cytokines. For each cytokine, the secretion was calculated as the percentage of cytokine secreting cells among CD4+ and CD8+ T cells. Variation of cytokine secretion for myeloid, CD4+ and CD8+ cells after *C. albicans* challenge. The frequencies of secreted cytokines for each immune cell population was compared to the frequencies of unstimulated cells on day 0 according to the ANOVA model. The fraction of inter-subject variability (white boxes) and *C. albicans* challenge variability (black boxes) were calculated and expressed as the total sum-of-squares, $n = 16$, $p \leq 0.05$. The inter-subject variability was quantified within the columns as the sum of squares of differences between each subject and the sixteen subjects mean. The post-challenge variability was quantified as the sum of squares of the differences between the column means and the grand mean. The F ratio was the ratio of two sum of square values. Large F ratio signified higher post-challenge variability than inter-subject variability. The *P* value was determined from the F ratio and the two values of degrees of freedom. Immune cells frequencies data were analyzed according to UI controls, CI and PI outcomes. $^{*}P < 0.05$; $^{**}P < 0.001$; $^{***}P < 0.0001$; $^{****}P < 0.00001$; ns = not significant.

	Myeloid cells						CD4+ T cells						CD8+ T cells					
	UI		CI		PI		UI		CI		PI		UI		CI		PI	
	F ratio	*P*	F ratio	*P*	F ratio	*P*	F ratio	*P*	F ratio	*P*	F ratio	*P*	F ratio	*P*	F ratio	*P*	F ratio	*P*
IFNγ	46.38	<0.0001	8.80	0,0003	12.77	0.0001	4.78	0.0085	3.39	0.0324	1.90	0.1524	2.71	0.0648	3.38	0.0327	1.78	0.1738
TNFα	6.79	0.0015	22.00	<0,0001	4.82	0.0141	3.45	0.0359	15.50	0.0001	3.70	0.0340	4.51	0.0143	1.29	0.2977	30.77	0.0001
IL-17	27.98	<0.0001	1.57	<0,0001	2.74	0.0827	0.99	0.4178	2.21	0.1110	1.86	0.1823	2.26	0.1125	0.17	0.9155	2.68	0.0870
IL-10	47.60	<0.0001	14.73	<0,0001	13.86	0.0001	3.37	0.0529	4.17	0.0150	4.19	0.0144	0.49	0.6937	1.44	0.2527	1.37	0.2735
IL-4	17.40	<0.0001	21.72	<0,0001	7.59	0.0030	2.70	0.0733	15.85	0.0001	7.65	0.0029	0.66	0.5860	209	0.1248	4.78	0.0169

Table 1. One-way ANOVA analysis of the human cytokine secretion variability after challenge by *C. albicans*. F: F ratio of post-challenge variability over inter-subject variability. UI: Uninfected cells, CI: Controlled infection outcome, PI: Persistent-infection outcome. *P* value: <0.05 was significant.

only because of fungus-mediated damage but also because of host-mediated damage or both, research efforts into the pathophysiology of human *C. albicans* infections should include the understanding of fungal pathogenicity in the context of the specific patient's immune response.

The major goal of this study was to probe the relevance of the *C. albicans* persistence model to monitor the dynamics of fungal and human immune cell interactions. To begin to model these complex interactions, we took into account the diversity of human immune responses after *C. albicans* challenge (subject-to-subject variability) and the temporal changes around the baseline parameters for each subject (within subject variability). The tSNE algorithm is a powerful data visualization and hypothesis generation technique. In order to visualize large datasets from multiple measurements, we integrated the tSNE algorithm to the study of the diversity of *C. albicans* persistence abilities during the interaction with immune cells. To our knowledge, this is the first study investigating the intra- and inter-individual diversity of human innate and adaptive immune responses against the diversity of *C. albicans* isolates. The input factors were normalized between uninfected and *Candida*-infected conditions in order to compare relative immune cell abundance and cytokine secretion. In the presence of highly conserved tSNE signatures for each subject over the sampling time period, our results allowed us to formulate hypothesis about the phenotypic modification induced after *C. albicans* challenge.

The frequencies of human blood leucocyte cell surface and functional markers were assessed in 16 subjects before and after challenge with three different *C. albicans* clinical isolates. By including the effect of baseline differences across subjects and their temporal changes around the baseline for each subject, we identified major temporal and quantitative intra-species differences concerning the ability of *C. albicans* to proliferate and persist despite the presence of immune cells. The analysis of both global CI and PI outcomes highlights significant differences between clinical isolates of *C. albicans*. In the context of intra- and inter-subject responses, we proposed the calculation of a persistence index for each clinical isolate at the scale of a group of subjects over the time correspond to its ability to proliferate and persist. In the literature, little attention has been given to the diversity of responses that the same clinical isolate could drive at the scale of one individual or a group of subjects. These results are consistent with previous works showing that the intra-species phenotypic and genetic adaptations of *C. albicans* exist and modulate immune recognition[31,36,37]. Hence, variations across natural isolates have also been demonstrated *in vitro* and in animal models[31,37–39]. Moreover, previous studies have shown that the loss of heterozygosity, aneuploidy, morphology and cell wall component changes are key contributors of the phenotypic plasticity of *C. albicans* during infection, supporting the observed differences in fungal persistence profiles into leucocyte co-cultures[36,37]. In contrast to previous *in vitro* models using unicellular co-cultures, the analysis of host-*Candida* interactions in human multicellular white blood cell co-cultures seems to be relevant to investigate such complex interactions, owing to differences between models[37].

Using the *C. albicans* persistence model integrated into tSNE algorithms, we have gone to the development of a framework transforming multiple data sets from the human immune responses, subjects and fungal isolate natural variations into comprehensive host-*C. albicans* signatures. The expression of immune cell surface markers at baseline was characterized by significant temporal stability within the subjects. The variance of CD4+ and CD8+ T lymphocytes was significant between subjects in contrast to the high subject-to-subject stability of CD66+ and CD14+ innate cells. The clustering of immune cell surface markers by tSNE at baseline supported the presence of conserved signatures within the subjects but highly variable between the subjects. Despite substantial inter-subject differences in adaptive CD4+ and CD8+ T cells and a large stability of CD66+ and CD14+ myeloid cells at baseline, our experimental approach led to the detection of substantial phenotypical changes in immune cells after *C. albicans* challenge. The global post-challenge variance of innate CD66+ and CD14+ cells was significant, and the variance of CD4+ and CD8+ T cell marker frequencies was stable. These results confirmed the required activation of anti-*Candida* phagocytosis and killing effector mechanisms of neutrophils and macrophages and the presence of stable T cell-infiltrating populations over time in order to generate a protective adaptive response[40–44]. Our results are consistent with others showing the influence of mononuclear phagocyte recognition of *C. albicans* during innate and adaptive immune responses to intestinal fungi[45].Our analyses of the composition of post-challenge leucocyte co-cultures over time highlight that *C. albicans* persistence could be due to a rapid reduction of CD66+ and CD14+ cells by day 2 and a reduced CD4+/CD8+ ratio compared to the CI outcome. Despite substantial inter-subject variation of CD4+ and CD8+ T cells at baseline, we detected coherent changes in both frequencies and cytokine secretion profiles after *C. albicans* challenge. Prior studies have also suggested that inter-individual differences in white blood cells exists in humans, which are impacted by

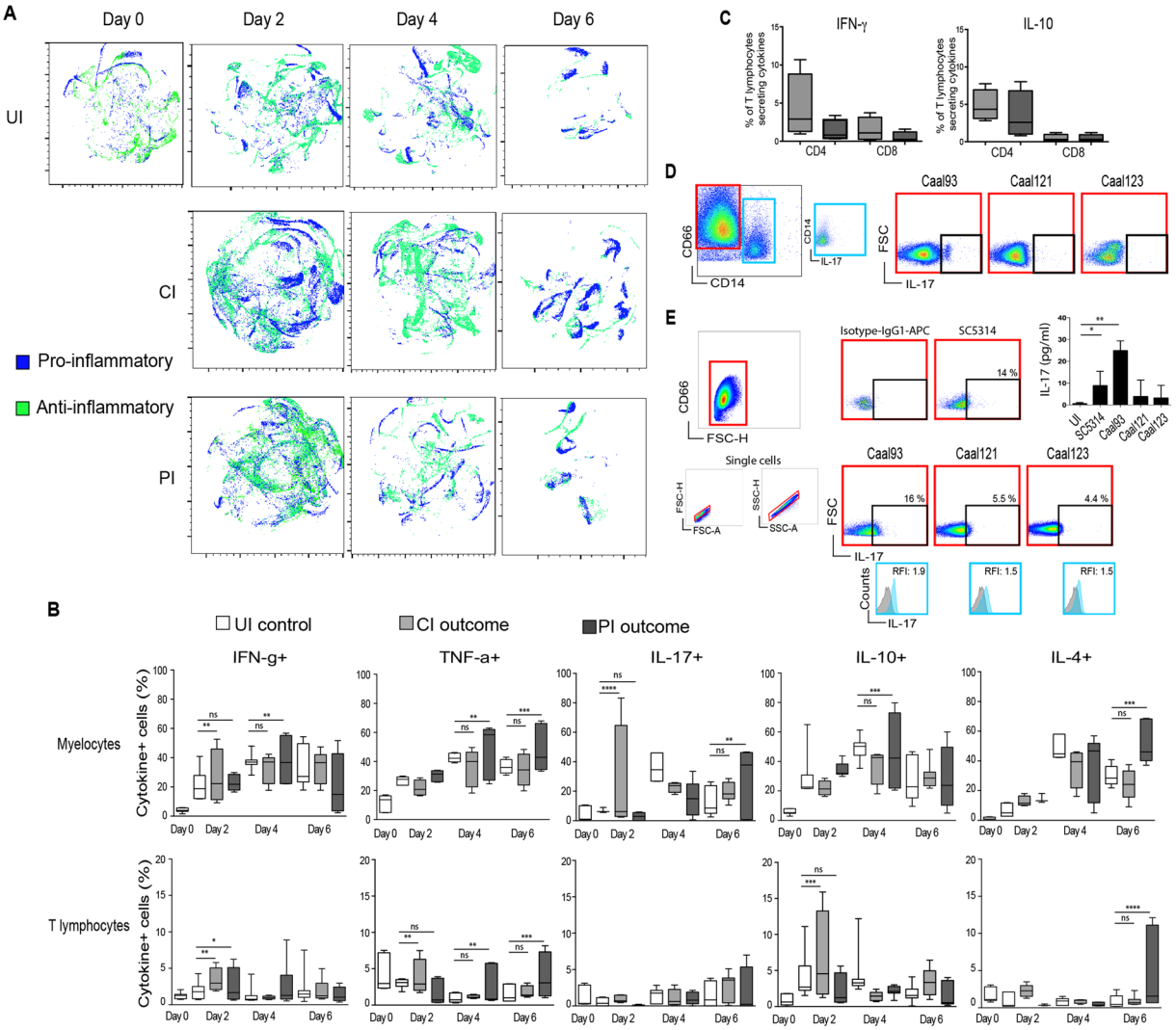

Figure 6. Cytokine secretion profiles after *C. albicans* challenge. (**A**) tSNE analysis of cytokine secretion variation in response to *C. albicans* challenge. After staining for CD4+, CD8+ membrane-antibody markers and for IFN-γ, TNF-α, IL-17, IL-10 and IL-4 secreted cytokines of unstimulated and *C. albicans*-stimulated leucocytes, cells were analyzed with FlowJo 10 for doublets, debris, and dead cells exclusion before gating living cells. Total pro-inflammatory (IFN-γ, blue) and anti-inflammatory (IL-10, green) cytokine expressing cells were concatenated and analyzed in tSNE module according to post-challenge time and to UI controls, CI and PI outcomes. (**B**) For each cytokine the secretion was analyzed as the percentage of cytokine secreting cells among myeloid cells and T lymphocytes. Box plots depict median, minimum and maximum percentages of immune cell frequencies according to UI controls (white boxes), CI (light gray) and PI (dark gray) outcomes for all of *C. albicans* clinical isolates ($n = 16$). (**C**) Percentage of CD4+ and CD8+ T lymphocyte secreting IFN-γ and IL-10 two days after *C. albicans* challenge. (**D**) Secretion of IL-17 by human CD66+ neutrophils into leucocyte co-cultures, two days after challenge by Caal93, Caal121 and Caal123 clinical isolates. (**E**) Gating strategy and analysis of Il-17 producing human neutrophils. CD66+ neutrophils were isolated by gradient centrifugation from three independent healthy volunteers. CD66+ cells were gated among sorted neutrophils cultures, followed by exclusion of doublets using forward scatter height (FSC-H) and forward scatter width (FSC-A). Caal93, Caal121, Caal123 and SC5314 *C. albicans* isolates were used to stimulate sorted neutrophils for 48 hours. The RFI was the ratio of the mean of fluorescence intensity (MFI) of *C. albicans*-stimulated neutrophils normalized to the MFI of respective IgG-isotype controls. IL-17 in supernatants of sorted neutrophils was quantified with a ProcartaPlex multiplex immunoassay kit (eBioscience). Concentrations were expressed as the mean ± SD of IL-17 in pg/ml of stimulated neutrophils among fungal isolates and uninfected controls ($n = 3$). *$P < 0.05$; **$P < 0.001$; ***$P < 0.0001$; ****$P < 0.00001$; ns = not significant.

environmental factors such as previous viral, fungal or bacterial infections or by genetic factors[46,47]. Nevertheless, consistent patterns after *C. albicans* challenge were only possible taking into account the outcome of the infection, strongly suggesting that both fungal and immune components should be considered. Analysis of multiple data sets before and after infection could reflect innate immune activation and adaptive changes specific to fungal

challenge. Nonetheless, our results suggest that anti-*Candida* responses also seem to be intimately linked to the baseline status of CD66+ neutrophil frequencies of each subject.

Given that the dimensionality reduced data suggested the presence of different cell subsets, we next evaluated functional changes in the secretion of cytokines by immune cells across subjects. With regard to the current knowledge about the essential role of cytokines during fungal infections, we also observed that *C. albicans* challenge induced a myriad of pro- and anti-inflammatory cytokines[15,48–50]. This *C. albicans* persistence approach allowed the analysis of cytokine secretion according to innate myeloid cells and adaptive CD4+ and CD8+ T cells. The frequencies of cytokine expressing cells significantly varied across subjects but were conserved within subjects. Although there were variations across subjects, our approach provided time resolved data on the secretion of cytokines by cells, leading to the identification of specific signatures.

Fungal CI was associated with a rapid activation of myeloid cells secreting pro-inflammatory IFN-γ and IL-17 cytokines by day 2. A subset of CD4+ T cells also rapidly secreted significant levels of IFN-γ and TNF-α. A CD4+ T cell subset secreted the anti-inflammatory IL-10 at the same time point. The secretion of IL-4 was not significantly different compared to uninfected cells. *C. albicans* PI was characterized by delayed secretion of IFN-γ, TNF-α, IL-17, IL-4 and IL-10 cytokines until days 4 and 6 after challenge. These cytokines were principally secreted by myeloid cells. TNF-α and IL-4 secreting CD4+ and CD8+ T cells were only significantly detected by days 4 and 6 after challenge compared to uninfected cells. According to our previous work, showing that the CD4hiCD8lo and CD4loCD8hi T cell subsets also secreted IL-4 and IL-10 cytokines under PI conditions, these results suggest that the secretion of delayed pro- and anti-inflammatory cytokines favoured fungal persistence[32].

Like other clinical and experimental studies, our results confirmed that CD66+ neutrophils and CD14+ macrophages are integral components of the innate immune system during *C. albicans* infection, leading to the activation and differentiation of Th cells[6,41,51–53]. Other studies have shown that myeloid cells control the elimination of *C. albicans* in the bloodstream[54]. The significant reduction of the CD66+ neutrophil frequencies after *C. albicans* challenge is consistent with their classical killing functions[54,55]. However, the percentages of this population remained significantly higher during the first 2 days under the CI compared to PI conditions, suggesting that their presence is important to drive appropriate anti-*C. albicans* responses. Interestingly, at the same time point, significant levels of IL-17 were secreted by CD66+ cells after challenge with the less persistent *C. albicans* isolate. Even if neutrophils themselves are a source of IL-17 during *Aspergillus* sp. and *Fusarium* sp. localized infections[56], there is no evidence for direct Il-17 secretion by neutrophils during oropharyngeal candidiasis[57]. Systemic candidiasis also has an IL-17 component; however, Th1 and NK cells secrete IFN-γ playing a relatively more important role[58]. Hence, IL-17 secretion by neutrophils during fungal infections seems to be conditioned by specific fungal and pathophysiologic compartments. Our results suggest that IL-17 secretion by neutrophils could be dependent upon the phenotypic characteristics of fungal isolates and would take a specific part among the main CD4+ Th17 cells and other IL-17 producers, such as ILC3, NK and NKT cells in innate immune populations[59–63]. These observations open a challenging question that has never been stated in the literature in the perspective of candidiasis. The understanding of this unusual IL-17 secretion by CD66+ cells in the context of *Candida* requires further mechanistic approaches, while these cells have been reported to express IL-17 during *Aspergillus*, *Fusarium* and *Mycobacterium tuberculosis* infections[56,64]. Moreover, neutrophils primed by IL-17 during *Candida* sepsis and kidney infection, promote early and sustained recruitment of other neutrophils[58,65].

The secretion of IFN-γ by CD4+ T cells is essential for an optimal activation of phagocytes, promoting optimal fungal clearance[6]. In the absence of significant secretion of IL-17 by CD4+ T cells in favour of significant IFN-γ secretion, our results suggest a Th1 response signature when infection was controlled. However, we cannot exclude the effect of other cellular sources of IL-17 production in our model[59–62]. Consistent with previous reports, the rapid secretion of IL-10 is necessary to dampen the pro-inflammatory effect of the IFN-γ driven Th1 response[6,66]. Our results have shown that the secretion of IL-10 by CD4+ T cells was early and then drastically reduced in days 4 and 6 after challenge. Myeloid cells also drove IL-10 secretion, but their frequencies were not significantly different compared to uninfected cells.

In contrast, *C. albicans* persistence induced a delayed myriad of pro- and anti-inflammatory cytokines, principally driven by myeloid cells. Previous clinical studies suggest that the inverse relationship between IFN-γ and IL-10 may correlate with a marked susceptibility to fungal infections, especially in those patients with significant levels of IL-10[67]. Macrophages differentiate into pro-inflammatory activated subtype M1 in response to *Candida* infections. Consistent with other studies and within the time frame of our assay, results suggest a M1-to-M2 switch that could contribute to *Candida* persistence by decreasing the type of immune response, therefore allowing fungal proliferation[68]. M2 macrophages are able to secrete high levels of IL-10 and IL-4[69–71]. Moreover, *C. albicans* persistence was associated with a delayed Th2 response. The IL-4 secretion signalled Th2-dependent inflammation, and its inhibition resulted in the restoration of antifungal responses[72].

Similar blood-immune cell experimental models have been used to analyse host-pathogen interactions to identify virulence factors and to test therapeutic approaches[42,73–75]. One major limitation of our approach is that many parameters of immune cell function and renewal from lymphoid organs remain inaccessible to direct quantification due to experimental isolation procedures. In contrast, the collection of blood samples remains relatively non-invasive and easy to perform. Because the blood cells circulate through all the tissues, these cells are exposed to stimuli and may reflect systemic changes.

Taken together, this experimental and analytical approach is available for the monitoring of such fungal and human immune responses. In the presence of genetic and non-genetic variations in human immune cells, this study also highlights that phenotypic variations within *C. albicans* isolates could contribute to the diversity of immune responses. Despite the subject-to-subject variability, the *Candida* persistence index and anti-fungal immune signatures can be modelled by this approach. This study also pointed out that these signatures are highly stable at an individual scale but must be analysed in the context of the multicellular and non-linear cytokine secretion kinetics. This study leads to a more comprehensive time-resolved and quantitative understanding of

how *Candida* and immune cells interact moving forward to a platform identification of fungal and human indicators of persistence. These observations have implications for both prevention and therapeutic perspectives.

Methods

Analysis of *C. albicans* persistence in co-culture with human leucocytes. Blood samples were obtained from sixteen healthy volunteers by venipuncture. Three independent blood samples were obtained from each subject to evaluate the intra and inter-individual variation of immune composition as previously described[32]. Briefly, peripheral blood mononuclear cells (PBMC) and polymorphonuclear neutrophils (PMN) were subsequently separated by dextran sedimentation (Dextran 500, 8% (w/v), density 1.113 ± 0.001 g/ml) followed by gradient centrifugation (dextran:blood ratio of 1:1). PBMC and PMN cell suspensions were washed twice in RPMI 1640, 8% human serum (HS) by centrifugation. Total leucocytes were adjusted to a final concentration of 2.5×10^6 cells/ml and cultured in RPMI 1640, 8% HS in 24-well tissue culture plates. Freshly cells were immediately infected by three *C. albicans* clinical isolates Caal93, Caal121 and Caal123 from the Mycobank of the Parasitology and Medical Mycology Department, Nantes, France at a monocyte:blastoconidia ratio of 2000:1. Co-cultures were incubated at 37 °C, 5% CO_2. Uninfected leucocytes were used as control of cellular reaction. The fungal burden within leucocyte cocultures was followed by colony-forming units calculation and human immune cell composition was analyzed over time by flow cytometry on days 0, 2, 4 and 6 post-infection. The total number and viability of cells at each time point was assessed by cell counting in the presence of 0.5% eosin.

To validate the IL-17 production by human neutrophils, these cells were sorted from peripheral blood cell samples from three healthy subjects by gradient sedimentation according to protocols[30]. The higher band of PBMC was separated from a lower one of neutrophils. Fresh separate neutrophil and PBMC fractions were simulated with *C. albicans* strains for two days.

For determination of growth rates, *C. albicans* clinical isolates were grown overnight at 30 °C in liquid YPD medium. 10^3 yeasts/ml were suspended in fresh RPMI 1640, 8% HS medium and incubated at 37 °C, 5% CO_2 over 12 hours. Growth rates were determined by measuring OD_{600} every two hours. The doubling time was calculated using the OD_{600} at 12 hours (T1) compared to h = 0 (T2) as following: $\ln 2 \times 60/((\ln OD_{600}$ of T1 $- \ln OD_{600}$ of T0)/12).

Ethics statement. Healthy volunteers were enrolled by the Blood Bank Center (Etablissement Français du Sang Pays de Loire, France, EFS)[32]. All blood samples were approved by the Ethics committee of the EFS Blood Bank Center with written informed consent obtained for all the donors, in accordance with the Declaration of Helsinki. Blood samples were transported from the EFS Blood Bank Center to the Nantes Université (EA1155 lab) within 30 minutes of drawing for PBMC isolation and *in vitro* studies, in accordance to the approved protocols (NTS-2013-02 and CPDL-PLER-2018-015).

Colony-forming unit assay. The *Candida* growth was measured by counting the living yeasts with a colony-counting technique (colony-forming unit, CFU) at different time periods (0, 2, 4 and 6 days post-challenge)[32]. After elimination of the supernatant, cells were washed twice in RPMI 8% HS and cell layers were gently scraped. Cell suspensions were homogenized by pipetting and several dilutions of each well (two wells per point) were plated on Potato-Dextrose Agar plates (PDA). After incubation during 24 to 48 hours at 30 °C, *Candida* colonies were counted. Data were expressed in CFU/ml and corresponded to the fungal burden of both yeasts within immune infiltrate structures and for filamentous species, after hyphae formation.

Staining of membrane antigen-specific leucocytes by flow cytometry. Flow cytometry procedures were followed as previously[32]. After elimination of the cell culture supernatant, cocultures were washed twice in PBS at 37 °C. Leucocyte cocultures were dispersed by pipetting and the total number of living cells at each time point was assessed by cell counting in the presence of 0.5% eosin. After single living cell gating, the mean percentages of viable cells varied between 85 to 95% for all samples. The analyses of cell population changes were based on the relative abundance of each cell subset within the total population of viable cells at each time point. The relative abundance of these subsets in uninfected controls was compared to *Candida* infected conditions in order to evaluate the impact of cell death on cell frequencies. To reduce technical variation during preanalytical procedures, we strictly followed protocols for tracking and processing fresh blood samples. We also verified repeatability of flow cytometry measurements based on the mean of fluorescent intensity (MFI) of time points over three months and using technical replicates for the same individual. The cells were suspended in 250 µl of PBS-BSA 1% and stained with a cocktail of fluorescent-conjugated antibodies in PBS-BSA 0.1%. The antibodies were specific to CD3-VioGreen (clone REA613, dilution 1/11, MACS Miltenyi Biotec), CD4-VioBright-FITC (clone REA623, dilution 1/11, MACS Miltenyi Biotec), CD8-PE (clone REA734, dilution 1/50, MACS Miltenyi Biotec), CD14-APC-Vio770 (clone TÜk4, MACS Miltenyi Biotec) and CD66abce-PE-Vio770 (clone TET2, MACS Miltenyi Biotec). These REA antibodies are recombinant human IgGs that display negligible binding to Fc receptors. Stain specificity was verified with isotypes-matched control antibodies VioBright-FITC-conjugated IgG1, VioBlue-conjugated IgG1, APC-conjugated IgG1, PE-conjugated IgG1. Cells were incubated for 1 h at 4 °C in the dark, washed twice with PBS and analyzed by flow cytometry. After gating on CD3 lymphocytes, the CD3+ population was separated into CD4+ and CD8+ T cells. CD66+ neutrophils and CD14+ monocytes came from granulocyte and monocyte regions. All data were acquired using the flow cytometer LSRII (BD Biosciences) and analyzed with FlowJo software version 10 (FlowJo) and FACSDIVA software version 8.0.1 (BD Biosciences) to separate the different cell subsets constituting *C. albicans* – leucocyte cocultures.

Cytokine secretion analysis by flow cytometry. IFN-γ, IL-17, IL-4, TNF-α and IL-10 producing cells were isolated by cytokine secretion assay (Miltenyi Biotec, Auburn, CA)[32]. Cocultures were washed, resuspended by pipetting and labeled with IFN-γ, IL-17, IL-4, TNF-α or IL-10 Catch Reagent (5 min on ice) and then incubated for 45 min at 37 °C in warm RPMI medium under slow continuous rotation. After washing with cold buffer, cells were labeled with PE-conjugated IL-10 detection antibody (10 µl label/10^6cells) and APC-conjugated IFN-γ detection antibody (10 µl label/10^6cells), PE-conjugated IL-4 and APC-IL-17 detection antibody and PE-TNF-α detection antibody. Isolated cells were counterstained using VioBlue-labeled anti-CD8 antibody (clone REA734), PE-Vio770-labeled anti-CD4 antibody (clone REA623), APC-Vio770-labeled anti-CD14 antibody (clone REA599) and PE-Vio770-labeled anti-CD66abce (clone TET2) before analyzing by flow cytometry. A human CytoStim (Miltenyi) was used as positive control of leucocyte activation and cytokine secretion at each time point. The analyses of changes in cytokine secretion by viable cells were based on the relative secretion by specific cell populations at each time point. The relative cytokine secretion in uninfected controls was compared to *Candida* infected conditions in order to evaluate the impact of cell death on cytokine secretion over the time[32]. The relative IL-17 secretion by sorted neutrophils was measured as the mean of fluorescence intensity (MFI) in arbitrary units and the ratio of fluorescence intensity (RFI) corresponding to the MFI of *C. albicans*-stimulated neutrophils normalized to the MFI of respective IgG-isotype controls. IL-17 in supernatants of sorted neutrophils was quantified with a ProcartaPlex multiplex immunoassay kit according to the manufacturer's instructions (eBioscience)[29].

T-distributed stochastic neighbor embedding analyses. After acquisition using flow cytometer LSRII, measured parameters were normalized and randomized. Data were first analyzed using FlowJo software. After doublets, debris, and dead cells excluding, living cells were gated. Downsampling function of multiple intra- and interindividual measurements was applied before data concatenation. Resulting FCS files were analyzed with the tSNE module. Specific plots were generated by healthy subject in order to analyze the intra-individual phenotype of cell populations, and between subjects to modeling global immune responses to *C. albicans*. Specific analyses by *C. albicans* isolate was also realized. The following input settings were used before tSNE reduction: up to 300,000 concatenated cells per file, 1000 iterations, 20 perplexity, 0.5 Theta. Pairwise comparations of all events were mapped in a low dimension space, arranging similar events nearby and dissimilar cells farther away. Cells were clustered by CD3, CD4, CD8, CD14 and CD66 expression. Specific tSNE analyzes were realized comparing IFN-γ pro-inflammatory and IL-10 anti-inflammatory cytokines[32]. Concatenated and individual experimental data were identically gated in FlowJo and statistics were analyzed with GraphPad Prism version 6.

Statistics. Statistical analyses were all carried out with Prism V6.0a software (GraphPad Software). The fungal burdens 6 days after challenge with each *Candida* isolate were compared using a two-way ANOVA test with Tukey's correction for multiple comparisons as previously described[32]. For the quantification of intra- and inter-subject variability at baseline, we pooled data from all individuals and we used a data vector $X = \{x_{st}\}$ (individual s, time-point t) where each x_{st} was associated with a subject and each subject had a total three measurements obtained from each of the time-points. Then we used the ANOVA model to evaluate the total variance (total sum of squares), subject-to-subject differences (between column variation) and the fraction of variance explained by subject relative to the residual of the fit. We also fitted an ANOVA model for the analysis of post-challenge variability. The surface immune cell markers and cytokine secreting cells were expressed in percentage. The inter-subject variability was quantified within the columns as the sum of squares of differences between each subject and the sixteen subjects mean. The post-challenge variability was quantified as the sum of squares of the differences between the columns means and the grand mean. The F ratio was the ratio of two sum of squares values. P values < 0.05 from ANOVA model indicated significant differences in cytokine secretion frequencies compared to the baseline (day 0). A F ratio was also calculated by computing respective *C. albicans* strain to inter-subject mean square values in order to assess how these parameters influence cytokine secretion. Large F ratio signified higher post-challenge variability than inter-subject variability. The *P* value was determined from the F ratio and the two values of degrees of freedom. The immune composition and cytokine kinetics of leucocyte cocultures was analyzed by one-way ANOVA with Tukey's correction for multiple comparisons. *P* values of ≤ 0.05 were considered significant.

Received: 26 July 2019; Accepted: 30 March 2020;
Published online: 10 April 2020

References

1. Dadar, M. *et al*. Candida albicans - Biology, molecular characterization, pathogenicity, and advances in diagnosis and control - An update. *Microb Pathog* **117**, 128–138 (2018).
2. Underhill, D. M. & Pearlman, E. Immune Interactions with Pathogenic and Commensal Fungi: A Two-Way Street. *Immunity* **43**, 845–858 (2015).
3. Perez, J. C., Kumamoto, C. A. & Johnson, A. D. Candida albicans commensalism and pathogenicity are intertwined traits directed by a tightly knit transcriptional regulatory circuit. *Plos Biol* **11**, e1001510 (2013).
4. Allert, S. *et al*. Candida albicans-Induced Epithelial Damage Mediates Translocation through Intestinal Barriers. *MBio* **9** (2018).
5. Richardson, J. P., Moyes, D. L., Ho, J. & Naglik, J. R. Candida innate immunity at the mucosa. *Semin. Cell Dev. Biol*., https://doi.org/10.1016/j.semcdb.2018.02.026 (2018).
6. Romani, L. Immunity to fungal infections. *Nat. Rev. Immunol.* **11**, 275–288 (2011).
7. Bitar, D. *et al*. Population-based analysis of invasive fungal infections, France, 2001-2010. *Emerg Infect Dis* **20**, 1149–1155 (2014).
8. Pfaller, M. A. *et al*. Epidemiology and outcomes of invasive candidiasis due to non-albicans species of Candida in 2,496 patients: data from the Prospective Antifungal Therapy (PATH) registry 2004-2008. *PLoS ONE* **9**, e101510 (2014).

9. Pfaller, M. A., Moet, G. J., Messer, S. A., Jones, R. N. & Castanheira, M. Candida bloodstream infections: comparison of species distributions and antifungal resistance patterns in community-onset and nosocomial isolates in the SENTRY Antimicrobial Surveillance Program, 2008-2009. *Antimicrob Agents Chemother* **55**, 561–566 (2011).
10. Segal, B. H. *et al*. Defining responses to therapy and study outcomes in clinical trials of invasive fungal diseases: Mycoses Study Group and European Organization for Research and Treatment of Cancer consensus criteria. *Clin Infect Dis* **47**, 674–683 (2008).
11. GAFFI. Global action fund for fungal infection; http://www.gaffi.org/ GAFFI (2014).
12. Yapar, N. Epidemiology and risk factors for invasive candidiasis. *Ther Clin Risk Manag* **10**, 95–105 (2014).
13. Arendrup, M. C. Epidemiology of invasive candidiasis. *Curr Opin Crit Care* **16**, 445–452 (2010).
14. Wang, X., van de Veerdonk, F. L. & Netea, M. G. Basic Genetics and Immunology of Candida Infections. *Infect Dis Clin North Am* **30**, 85–102 (2016).
15. Netea, M. G., Joosten, L. A. B., van der Meer, J. W. M., Kullberg, B.-J. & van de Veerdonk, F. L. Immune defence against Candida fungal infections. *Nat. Rev. Immunol.* **15**, 630–642 (2015).
16. Borghi, M. *et al*. Pathogenic NLRP3 Inflammasome Activity during Candida Infection Is Negatively Regulated by IL-22 via Activation of NLRC4 and IL-1Ra. *Cell Host Microbe* **18**, 198–209 (2015).
17. Martinez-Alvarez, J. A., Perez-Garcia, L. A., Flores-Carreon, A. & Mora-Montes, H. M. The immune response against Candida spp. and Sporothrix schenckii. *Rev Iberoam Micol* **31**, 62–66 (2014).
18. Hope, W., Natarajan, P. & Goodwin, L. Invasive fungal infections. *Clin Med (Lond)* **13**, 507–510 (2013).
19. Kim, M. H. *et al*. Neutrophil survival and c-kit(+)-progenitor proliferation in Staphylococcus aureus-infected skin wounds promote resolution. *Blood* **117**, 3343–3352 (2011).
20. Gow, N. A., van de Veerdonk, F. L., Brown, A. J. & Netea, M. G. Candida albicans morphogenesis and host defence: discriminating invasion from colonization. *Nat Rev Microbiol* **10**, 112–122 (2012).
21. Jabra-Rizk, M. A. *et al*. Candida albicans Pathogenesis: Fitting within the Host-Microbe Damage Response Framework. *Infect Immun* **84**, 2724–2739 (2016).
22. Aoun, J. *et al*. Caseating granulomas in cutaneous leishmaniasis. *PLoS Negl Trop Dis* **8**, e3255 (2014).
23. Girgis, N. M. *et al*. Ly6C(high) monocytes become alternatively activated macrophages in schistosome granulomas with help from CD4+ cells. *PLoS Pathog* **10**, e1004080 (2014).
24. Subbian, S. *et al*. Lesion-Specific Immune Response in Granulomas of Patients with Pulmonary Tuberculosis: A Pilot Study. *PLoS ONE* **10**, e0132249 (2015).
25. Heninger, E. *et al*. Characterization of the Histoplasma capsulatum-induced granuloma. *J Immunol* **177**, 3303–3313 (2006).
26. De Luca, A. *et al*. IL-22 and IDO1 affect immunity and tolerance to murine and human vaginal candidiasis. *PLoS Pathog* **9**, e1003486 (2013).
27. Legrand, F. *et al*. Adjuvant corticosteroid therapy for chronic disseminated candidiasis. *Clin Infect Dis* **46**, 696–702 (2008).
28. Singh, H. R., Singh, N. G. & Singh, T. B. Estimation of CD4+ and CD8+ T-lymphocytes in human immunodeficiency virus infection and acquired immunodeficiency syndrome patients in Manipur. *Indian J Med Microbiol* **25**, 126–132 (2007).
29. Misme-Aucouturier, B., Albassier, M., Alvarez-Rueda, N. & Le Pape, P. Specific Human and Candida Cellular Interactions Lead to Controlled or Persistent Infection Outcomes during Granuloma-Like Formation. *Infect Immun* **85**, e00807–16 (2017).
30. Alvarez-Rueda, N. *et al*. First human model of *in vitro* Candida albicans persistence within granuloma for the reliable study of host-fungi interactions. *PLoS ONE* **7**, e40185 (2012).
31. Schönherr, F. A. *et al*. The intraspecies diversity of C. albicans triggers qualitatively and temporally distinct host responses that determine the balance between commensalism and pathogenicity. *Mucosal Immunol* **10**, 1335–1350 (2017).
32. Misme-Aucouturier, B. *et al*. Double positive CD4+CD8+ T cells are part of the adaptive immune response against Candida albicans. *Hum. Immunol.* **80**, 999–1005 (2019).
33. Chen, E. *et al*. Fungal-Host Interaction: Curcumin Modulates Proteolytic Enzyme Activity of Candida albicans and Inflammatory Host Response *In Vitro*. *Int J Dent* **2018**, 2393146 (2018).
34. Rapala-Kozik, M. *et al*. Extracellular proteinases of Candida species pathogenic yeasts. *Mol Oral Microbiol* **33**, 113–124 (2018).
35. Trevino-Rangel, R. J. *et al*. Phenotypical characterization and molecular identification of clinical isolates of Candida tropicalis. *Rev Iberoam Micol* **35**, 17–21 (2018).
36. Hirakawa, M. P. *et al*. Genetic and phenotypic intra-species variation in Candida albicans. *Genome Res.* **25**, 413–425 (2015).
37. Marakalala, M. J. *et al*. Differential adaptation of Candida albicans *in vivo* modulates immune recognition by dectin-1. *PLoS Pathog* **9**, e1003315 (2013).
38. MacCallum, D. M. *et al*. Property differences among the four major Candida albicans strain clades. *Eukaryotic Cell* **8**, 373–387 (2009).
39. Netea, M. G. & Maródi, L. Innate immune mechanisms for recognition and uptake of Candida species. *Trends Immunol* **31**, 346–353 (2010).
40. Amulic, B., Cazalet, C., Hayes, G. L., Metzler, K. D. & Zychlinsky, A. Neutrophil function: from mechanisms to disease. *Annu. Rev. Immunol.* **30**, 459–489 (2012).
41. Fradin, C. *et al*. Granulocytes govern the transcriptional response, morphology and proliferation of Candida albicans in human blood. *Mol Microbiol* **56**, 397–415 (2005).
42. Hünniger, K. *et al*. A virtual infection model quantifies innate effector mechanisms and candida albicans immune escape in human blood. *PLoS Comput Biol* **10**, e1003479 (2014).
43. Ngo, L. Y. *et al*. Inflammatory monocytes mediate early and organ-specific innate defense during systemic candidiasis. *J Infect Dis* **209**, 109–119 (2014).
44. Romani, L. *et al*. Neutrophil production of IL-12 and IL-10 in candidiasis and efficacy of IL-12 therapy in neutropenic mice. *J Immunol* **158**, 5349–5356 (1997).
45. Leonardi, I. *et al*. CX3CR1+ mononuclear phagocytes control immunity to intestinal fungi. *Science* **359**, 232–236 (2018).
46. Zielinski, C. E. *et al*. Pathogen-induced human TH17 cells produce IFN-gamma or IL-10 and are regulated by IL-1beta. *Nature* **484**, 514–518 (2012).
47. Griffiths, S. J. *et al*. Age-associated increase of low-avidity cytomegalovirus-specific CD8+ T cells that re-express CD45RA. *J Immunol* **190**, 5363–5372 (2013).
48. van de Veerdonk, F. L., Joosten, L. A. & Netea, M. G. The interplay between inflammasome activation and antifungal host defense. *Immunol. Rev.* **265**, 172–180 (2015).
49. van de Veerdonk, F. L. *et al*. Protective host defense against disseminated candidiasis is impaired in mice expressing human interleukin-37. *Front Microbiol* **5**, 762 (2014).
50. van de Veerdonk, F. L. *et al*. Redundant role of TLR9 for anti-Candida host defense. *Immunobiology* **213**, 613–620 (2008).
51. Jacobsen, I. D., Luttich, A., Kurzai, O., Hube, B. & Brock, M. *In vivo* imaging of disseminated murine Candida albicans infection reveals unexpected host sites of fungal persistence during antifungal therapy. *J Antimicrob Chemother* **69**, 2785–2796 (2014).
52. Lionakis, M. S. *et al*. Chemokine receptor Ccr1 drives neutrophil-mediated kidney immunopathology and mortality in invasive candidiasis. *PLoS Pathog* **8**, e1002865 (2012).
53. Wozniok, I. *et al*. Induction of ERK-kinase signalling triggers morphotype-specific killing of Candida albicans filaments by human neutrophils. *Cell Microbiol* **10**, 807–820 (2008).

54. Hünniger, K. *et al*. A second stimulus required for enhanced antifungal activity of human neutrophils in blood is provided by anaphylatoxin C5a. *J Immunol* **194**, 1199–1210 (2015).
55. Lionakis, M. S. & Netea, M. G. Candida and host determinants of susceptibility to invasive candidiasis. *PLoS Pathog* **9**, e1003079 (2013).
56. Taylor, P. R., Leal, S. M., Sun, Y. & Pearlman, E. Aspergillus and Fusarium corneal infections are regulated by Th17 cells and IL-17-producing neutrophils. *J Immunol* **192**, 3319–3327 (2014).
57. Huppler, A. R., Verma, A. H., Conti, H. R. & Gaffen, S. L. Neutrophils Do Not Express IL-17A in the Context of Acute Oropharyngeal Candidiasis. *Pathogens* **4**, 559–572 (2015).
58. Huang, W., Na, L., Fidel, P. L. & Schwarzenberger, P. Requirement of interleukin-17A for systemic anti-Candida albicans host defense in mice. *J Infect Dis* **190**, 624–631 (2004).
59. Bacher, P. *et al*. Human Anti-fungal Th17 Immunity and Pathology Rely on Cross-Reactivity against Candida albicans. *Cell* **176**, 1340–1355.e15 (2019).
60. Mengesha, B. G. & Conti, H. R. The Role of IL-17 in Protection against Mucosal Candida Infections. *J Fungi (Basel)* **3**, 52 (2017).
61. Conti, H. R. & Gaffen, S. L. IL-17-Mediated Immunity to the Opportunistic Fungal Pathogen Candida albicans. *J Immunol* **195**, 780–788 (2015).
62. Bär, E., Whitney, P. G., Moor, K., Reise Sousa, C. & Leibundgut-Landmann, S. IL-17 regulates systemic fungal immunity by controlling the functional competence of NK cells. *Immunity* **40**, 117–127 (2014).
63. Atarashi, K. *et al*. Th17 Cell Induction by Adhesion of Microbes to Intestinal Epithelial Cells. *Cell* **163**, 367–380 (2015).
64. Hu, S. *et al*. IL-17 Production of Neutrophils Enhances Antibacteria Ability but Promotes Arthritis Development During Mycobacterium tuberculosis Infection. *EBioMedicine* **23**, 88–99 (2017).
65. Hernandez-Santos, N. & Gaffen, S. L. Th17 cells in immunity to Candida albicans. *Cell Host Microbe* **11**, 425–435 (2012).
66. Romani, L. & Puccetti, P. Controlling pathogenic inflammation to fungi. *Expert Rev Anti Infect Ther* **5**, 1007–1017 (2007).
67. Romani, L. & Puccetti, P. Protective tolerance to fungi: the role of IL-10 and tryptophan catabolism. *Trends Microbiol* **14**, 183–189 (2006).
68. Reales-Calderon, J. A., Aguilera-Montilla, N., Corbi, A. L., Molero, G. & Gil, C. Proteomic characterization of human proinflammatory M1 and anti-inflammatory M2 macrophages and their response to Candida albicans. *Proteomics* **14**, 1503–1518 (2014).
69. Vogel, D. Y. *et al*. Human macrophage polarization *in vitro*: maturation and activation methods compared. *Immunobiology* **219**, 695–703 (2014).
70. Ambarus, C. A., Noordenbos, T., de Hair, M. J., Tak, P. P. & Baeten, D. L. Intimal lining layer macrophages but not synovial sublining macrophages display an IL-10 polarized-like phenotype in chronic synovitis. *Arthritis Res. Ther.* **14**, R74 (2012).
71. Schraufstatter, I. U., Zhao, M., Khaldoyanidi, S. K. & Discipio, R. G. The chemokine CCL18 causes maturation of cultured monocytes to macrophages in the M2 spectrum. *Immunology* **135**, 287–298 (2012).
72. Szymczak, W. A. & Deepe, G. S. J. The CCL7-CCL2-CCR2 axis regulates IL-4 production in lungs and fungal immunity. *J Immunol* **183**, 1964–1974 (2009).
73. Echenique-Rivera, H. *et al*. Transcriptome analysis of Neisseria meningitidis in human whole blood and mutagenesis studies identify virulence factors involved in blood survival. *PLoS Pathog* **7**, e1002027 (2011).
74. Deslouches, B. *et al*. Activity of the de novo engineered antimicrobial peptide WLBU2 against Pseudomonas aeruginosa in human serum and whole blood: implications for systemic applications. *Antimicrob Agents Chemother* **49**, 3208–3216 (2005).
75. Tena, G. N. *et al*. Failure to control growth of mycobacteria in blood from children infected with human immunodeficiency virus and its relationship to T cell function. *J Infect Dis* **187**, 1544–1551 (2003).

Acknowledgements

We thank the healthy donors included in this study. We also thank the Cytometry Facility CytoCell for expert technical assistance (SFR François Bonamy, Nantes, France).

Author contributions

N.A.R. and P.L.P. conceived and designed the experiments. N.A.R., M.A., B.M.A., A.T. and C.R. performed the experiments. N.A.R. and P.L.P. analyzed the data. P.L.P. contributed reagents and materials tools. N.A.R. and P.L.P. wrote the paper.

Competing interests

The authors declare no competing interests.

Additional information

Correspondence and requests for materials should be addressed to N.A.-R. or P.L.P.

Reprints and permissions information is available at www.nature.com/reprints.

Publisher's note Springer Nature remains neutral with regard to jurisdictional claims in published maps and institutional affiliations.